Creating RNA Bulges: Cleavage of RNA in RNA/DNA Duplexes by Metal Ion Catalysis†

Dieter Hüsken,*,‡ Greg Goodall,§,⊥ Marcel J. J. Blommers,|| Wolfgang Jahnke,|| Jonathan Hall,‡ Robert Häner,‡ and Heinz E. Moser‡

Central Research Laboratories, Ciba-Geigy Ltd., CH-4002 Basel, Switzerland, Bio-NMR, Ciba-Geigy Ltd., CH-4002 Basel, Switzerland, and Friedrich Miescher Institute, Basel, Switzerland

Received July 11, 1996; Revised Manuscript Received October 3, 1996⊗

ABSTRACT: The manipulation of a single-stranded RNA target by forming different RNA/antisense hybrids demonstrates the possibility of cleaving the RNA strand within duplexes. This was achieved using the sequence composition of the antisense oligonucleotide, an approach that results in various bulges [unpaired base(s)] in the RNA target, which is then cleavable at these specific bulge sites under free metal ion or metal complex catalysis. RNA cleavages promoted by metal ions were performed under mild conditions and characterized by separating the RNA fragments carrying end label. The observed products result from intramolecular transesterification causing RNA strand scission. No detectable cleavage of the RNA was observed with either a fully complementary RNA/antisense hybrid or a bulged base in the antisense strand. A molecular modeling study of the RNA backbone suggests that the local conformation of the RNA backbone at a bulge in such hybrid duplexes greatly facilitates the metal-assisted catalytic cleavage. Endonucleolytic RNA cleavage within an RNA/antisense hybrid by metal complexes attached to the antisense oligonucleotide might lead to a new approach in antisense technology with artificial ribonucleases which operate with catalytic turnover.

A great deal of research activity is currently underway in antisense technology (Crooke, 1994; De Mesmaeker et al., 1995; Altmann et al., 1996). While several phosphorothioate oligonucleotides are under investigation in the clinic (Field & Goodchild, 1995), the search for a more potent class of antisense oligonucleotides continues. Particular interest in this respect is focused on artificial nucleases, which specifically cleave a given target RNA by mediating intramolecular transesterification at an internucleotide phosphodiester of the RNA. Macrocyclic lanthanide complexes linked to oligonucleotides are a noteworthy example (Magda et al., 1994; Matsumura et al., 1994; Hall et al., 1994; Häner et al., 1996).

The phosphodiester backbone of short single-stranded RNAs is generally free to fold and rotate without major conformational restrictions. Metal salts of magnesium and the lanthanides (Eichhorn & Butzow, 1965; Breslow & Huang, 1991; Kuusela & Lönnberg, 1994; Matsuo et al., 1995) as well as lanthanum complexes (Morrow et al., 1992; Hayashi et al., 1993; Schneider et al., 1993; Amin et al., 1994; Morrow & Shelton, 1994; Chin & Morrow, 1994) are known to accelerate the transesterification/cleavage reaction of RNA (J. Chin, personal communication, 1996).[2] However, unlike single-stranded RNA, double-stranded RNA is more resistant to cleavage (Gornicki et al., 1989; Kolasa et al., 1993). Even for enzymatic RNA cleavage, the topology of the helix prevents the intramolecular transesterification process. This is shown in Table 1, where the specific properties of natural nucleases which depend on substrates are noted. Single-strand specific ribonucleases and ribozymes (group 1 in Table 1) exclusively operate *via* the intramolecular 2′-transesterification mechanism. A second class of nucleases, including intermolecularly acting ribozymes, cleaves both single-stranded RNA and DNA and therefore employs either water or the hydroxyl group of a ribonucleotide as the nucleophile. Finally, the third group includes RNases specific to double-stranded RNA/DNA or RNA/RNA which also use water or hydroxide as the nucleophile. That this class of nucleases acts hydrolytically on an RNA substrate is at first sight surprising; nature does not take advantage of the neighboring 2′-hydroxyl group of the ribose to effect the cleavage intramolecularly, favoring instead direct nucleophilic attack at the phosphodiester by water. This is probably due to conformational restriction of the phosphodiester backbone in the double helix such that transesterification by 2′-OH cannot easily occur without major conformational rearrangement.

On the basis of this knowledge, we began our investigation with the aim of specifically cleaving RNA in an RNA/DNA helix by forcing the phosphodiester backbone of the RNA strand to adopt a favorable conformation for a catalyzed transesterification/cleavage reaction. This conformational

† This work was carried out at the Central Research Laboratories, Ciba-Geigy Ltd.

* Author to whom correspondence should be addressed.
‡ Central Research Laboratories, Ciba-Geigy Ltd.
§ Friedrich Miescher Institute.
|| Bio-NMR, Ciba-Geigy Ltd.
⊥ Present address: Hanson Centre for Cancer Research, Institute of Medical and Veterinary Science, Box 14, Rundle Street Post Office, Adelaide, South Australia 5000.

⊗ Abstract published in *Advance ACS Abstracts,* December 1, 1996.

[1] Abbreviations: ATP, adenosine 5′-triphosphate; EDTA, ethylenediaminetetraacetic acid; NMR, nuclear magnetic resonance; NTP, ribonucleoside triphosphate; nt, nucleotide; ODN, oligodeoxyribonucleotide; SDS, sodium dodecyl sulfate; Tris, tris(hydroxymethyl)aminomethane; Tris-HCl, Tris hydrochloride.

[2] Jik Chin, McGill University (1996), personal communication. The magnitudes of different rates of accelerating RNA cleavage promoted by metal ions and the reaction type are estimated at best as 10^9 for the intramolecular 2′-hydroxide attack, 10^8 for the metal hydroxide as the nucleophile, 10^6 for the leaving group activation, 10^3 for the metal hydroxide as general base for 2′-hydroxyl proton abstraction, and 10^2 for the Lewis acid activation of the phosphate.

S0006-2960(96)01700-X CCC: $12.00

Table 1: Nucleases and Ribozymes with Known Structures and a Well-Examined Reaction Mechanism[a]

group	enzyme	specificity	substrate	cofactor	first reaction step	product termini	references
I	RNase A	ss[b]	RNA	no metal ion	transesterification[c]	2′,3′-cp[b]	Borah et al., 1985; Eftink & Biltonen, 1983a−c; Cuchillo et al., 1993
I	RNase T_1	ss	RNA	no metal ion	transesterification[c]	2′,3′-cp	Arni et al., 1988; Winkler et al., 1993
I	internal nucleophile ribozyme e.g. hammerhead	ss	RNA	Mg^{2+} [f]	transesterification	2′,3′-cp	Pley et al., 1994; Scott et al., 1995
II	external nucleophile ribozyme e.g. *Tetrahymena* e.g. ribonuclease P RNA[g]	ss	RNA and DNA	Mg^{2+} [f]	hydrolysis[d]	5′-mp[b] 3′-hy[b,d]	Herschlag & Cech, 1990; Robertson & Joyce, 1990; Cech et al., 1992; Altman et al., 1993
II	staphylococcal nuclease (SNase)	ss and ds[b]	RNA and DNA	Ca^{2+}	hydrolysis	5′-hy 3′-mp	Cotton et al., 1979; Loll & Lattman, 1989
III	RNase H I (*E. coli*) HIV-1 reverse transcriptase RNase H domain	ds	RNA in RNA/DNA	Mg^{2+} [f]	hydrolysis[e]	5′-mp 3′-hy	Yang et al., 1990; Davies et al., 1991; Katayanagi et al., 1992
III	RNase V_1[h]	ds	RNA	Mg^{2+}	hydrolysis	5′-mp 3′-hy	Wyatt & Walker, 1989
III	RNase III[h]	ds	RNA	Mg^{2+} and Co^{2+} [f]	hydrolysis	5′-mp 3′-hy	Li et al., 1993; Hjalt & Wagner, 1995

[a] All listed enzymes are described with a catalysis pathway following the in-line mechanism. [b] Abbreviations: cp, cyclic phosphate; ds, double-strand; hy, hydroxyl; mp, monophosphate; ss, single-strand. [c] The second reaction step (hydrolysis) is also described as in-line (Eftink & Biltonen, 1983; Winkler et al., 1993). [d] 3′-OH of nucleoside G as a nucleophile in the case of *Tetrahymena* ribozyme (product; 3′,5′-diester). [e] Discussed are activated water from Asp as a general base (Oda et al., 1993) and activated water from two metal ions (Davies et al., 1991). [f] In addition, Mn^{2+}. [g] In addition, Ca^{2+}. [h] No X-ray structure known.

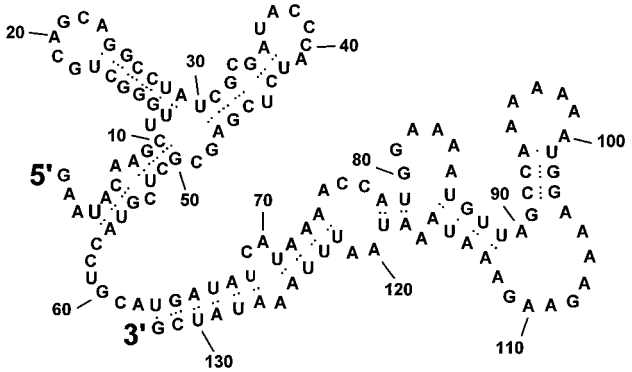

FIGURE 1: Sequence of the target RNA-1 with the position numbers and possible secondary structure as predicted by *FoldRNA* (Zuker, 1989) of the Genetics Computer Group WISCONSIN PACKAGE Version 8.0.

change was effected by the introduction of secondary-structure motifs such as mismatches and bulges in the RNA. The results of cleavage induced by metal ions and a lanthanide complex at these motifs are discussed in terms of structural and conformational considerations of the cleavage site.

MATERIALS AND METHODS

Preparation of Target RNA-1. The sequence of RNA-1 is shown in Figure 1. RNA-1 was synthesised by *in vitro* runoff transcription with SP6 RNA polymerase using *Cla*I-linearized plasmid pGS7 which contains a synthetic plant intron and the flanking synthetic exon sequence inserted as 172 base pairs of XbaI/PstI in the pGEM-1 (Promega) vector (Goodall & Filipowicz, 1989). The transcription reactions were carried out in 100 μL of 40 mM Tris-HCl (pH 7.5) containing 6 mM magnesium chloride, 2 mM spermidine, 10 mM sodium chloride, 10 mM dithiothreitol, each NTP (1 mM), 1 u/μL RNasin, 5 μg of DNA template, and 0.75 u/μL SP6 RNA polymerase. Reaction mixtures were incubated for 1 h at 37 °C. After phenol/chloroform/isoamyl alcohol (25:24:1, v/v/v) extraction and ethanol precipitation with 1 M ammonium acetate and 0.5 μg/μL glycogen (Renner), the RNA was washed twice with 70% ethanol.

Synthesis of Target RNA-2 (RNA/DNA Chimera). RNA-2 was 5′-d(CTAGCCGACTGC)r(CGAUCUC)d(GCCACTC-TAC). RNA-2 was synthesised by phosphoramidite chemistry on an ABI Model 380B synthesiser. To remove 2′-OH *tert*-butyldimethylsilyl protecting groups, the synthetic RNA-2 was dissolved in 0.3 mL of water, lyophilized, redissolved in 0.2 mL of 1 M tetrabutylammonium fluoride in tetrahydrofuran (Aldrich), kept overnight at 22 °C, subsequently mixed with 0.2 mL of 50 mM tetraammonium hydrogen carbonate at pH 8.0, and dialyzed against water.

Synthesis and Purification of Oligodeoxyribonucleotides (ODNs). The following is a list of ODNs used in this study: ODN-1, ATAGGCCTGCTGCAGCCCAAGCTTGTATTC; ODN-2, GATAGGCCTGCTGCTAGCCCAAGCTTGTAT-TC; ODN-3, GATAGGCCTGCTGCAGCCCAA#CTTGT-ATTC; ODN-4, GATAGGCCTGCTGC#GCCCAAGCTT-GTATTC; ODN-5, GATAGGCC#GCTGCAGCCCAAG-CTTGTATTC; ODN-6, CGCGAT#GGCC#GCTGC#GCC-CAA#CTTGTATTC; ODN-7, GATAGGCCTGCTGCA#C-CCAAGCTTGTATTC; ODN-8, CGATAGGCCTGCTGC-##CCCAAGCTTGTATTC; ODN-9, GC GATAGGCCTG-CTGCAGC###AGCTTGTATTC; ODN-10, CGCGATAG-GCCTGCTGCA####AAGCTTGTATTC; ODN-11, ATAG-GCCTGCTGCTGCCCAAGCTTGTATTC; ODN-12, AT-AGGCCTGCTGGTGCCCAAGCTTGTATTC; ODN-13, GA TAGGCCTGCTGCAGCC#AAGCTTGTATTC; ODN-14, GCGATAGGCCTGCT G###CCCAAGCTTGTATTC. O-DN-15, GTAGAGTGGCGAGATCGGCAGTGGGCTAG; ODN-16, GTAGAGTGGCG#GATCGGCAGTGGGCTAG; ODN-17, GTA GAGTGGCGAG##CGGCAGTGGGCTAG. Pound marks in the sequences of ODN-3−10, ODN-13, ODN-14, ODN-16, and ODN-17 indicate the positions of bulges induced in the RNA upon hybridization with RNA-1 or RNA-2, respectively (Figures 2 and 3). Also underlined are the additional base T in ODN-2 and the bases in ODN-

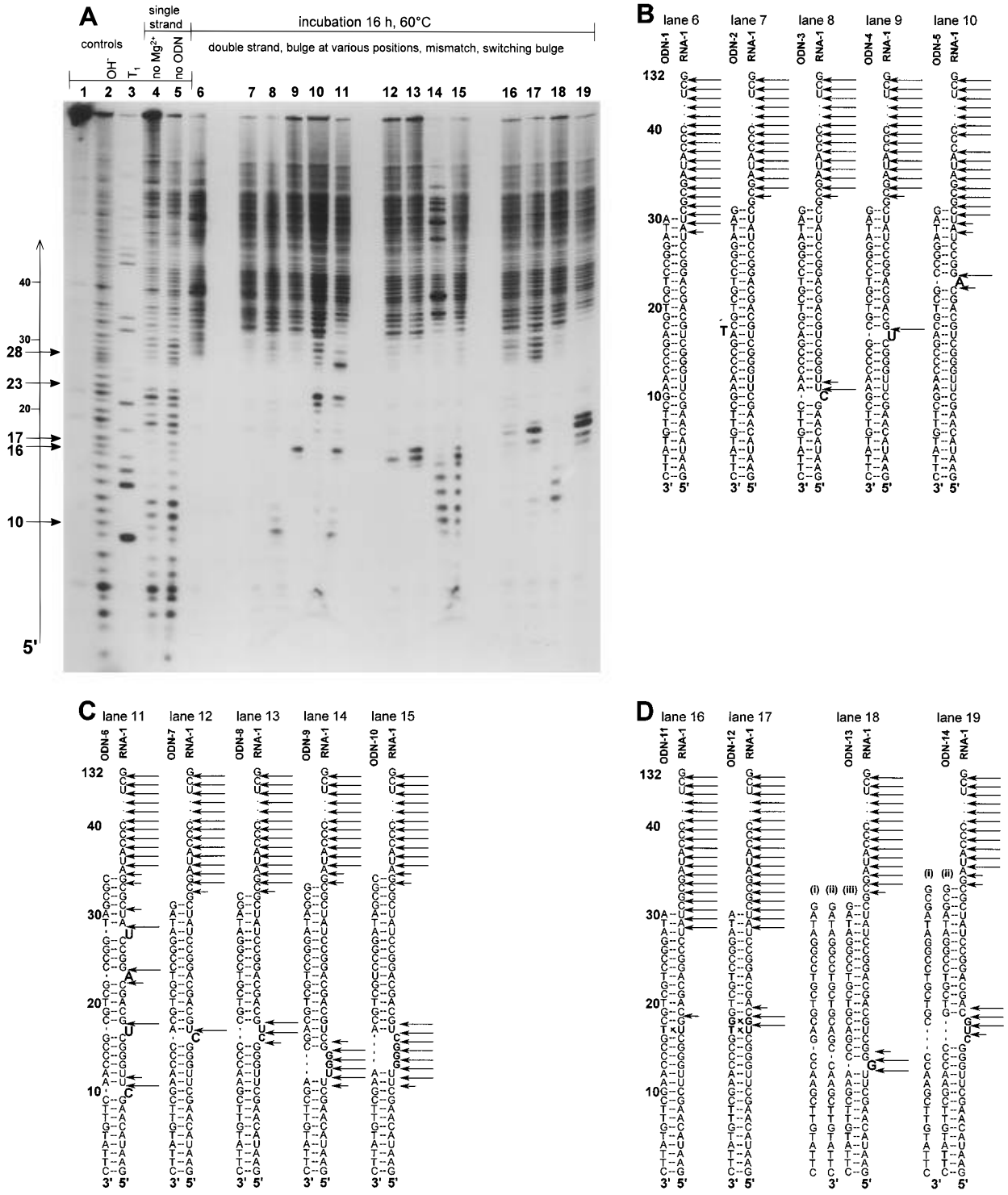

FIGURE 2: (A) Autoradiogram of a 6% denaturing polyacrylamide gel obtained after treatment of the RNA-1 (132 nt, 5′-^{32}P-labeled transcript) with or without magnesium ion in the presence of oligodeoxyribonucleotides (ODNs). The incubation was carried out at 60 °C for 16 h in a reaction mixture containing approximately 10−50 nM RNA-1 and 1 μM ODN in a buffer of 2.5 mM magnesium chloride, 100 mM sodium acetate, and 50 mM sodium borate at pH 8.0 in a total volume of 20 μL (lanes 5−19): lane 1, untreated transcript RNA-1; lane 2, partial alkaline hydrolysis (sodium hydrogen carbonate at pH 10 for 20 min at 70 °C); lane 3, partial digestion with RNase T1; lane 4, incubated without magnesium salt; and lane 5, no ODN added. In lanes 6−19, different ODNs were present: lane 6, ODN-1, 30 nt, fully complementary to the 5′-end of the transcript; lane 7, ODN-2, 32 nt, one bulge in the DNA strand at position 18; lane 8−10 and 12, ODN-3, ODN-4, ODN-5, and ODN-7, 31 nt, one bulge in the RNA strand at positions 10, 17, 23, and 16, respectively; lane 11, ODN-6, 34 nt, four single bulges at positions 10, 17, 23, and 28; lane 13, ODN-8, 32 nt, one double bulge at positions 16 and 17; lane 14, ODN-9, 33 nt, multiple bulge at positions 12−14; lane 15, ODN-10, 34 nt, multiple bulge at positions 13−16; lane 16, ODN-11, 30 nt, one mismatch at position 17; lane 17, ODN-12, 30 nt, two mismatches at positions 17 and 18; lane 18, ODN-13, 31 nt, one bulge possible at position 13, 14, or 15; and lane 19, ODN-14, 33 nt, one triple bulge possible at positions 15−17 or 16−18. The arrows indicates the bulge positions in lanes 8−13. (B−D) Schematic presentation of the observed magnesium salt-promoted cleavage of RNA-1 (shown in Figure 2A) with the same lane counting. The positions of the bases are numbered counting from the 5′-end of the RNA-1 target. The RNA cleavage sites are indicated by arrows of different lengths regarding the cleavage intensities at the bulges, mismatches, and the single-strand−double-strand junctions and for simplicity with one length in the single-strand region. Bulged bases are shown within the duplex region, and mismatches are illustrated with a cross. Different base pairings of ODN-13 and ODN-14 with RNA-1 are illustrated with (i), (ii), and (iii) defining possible positions of the bulge.

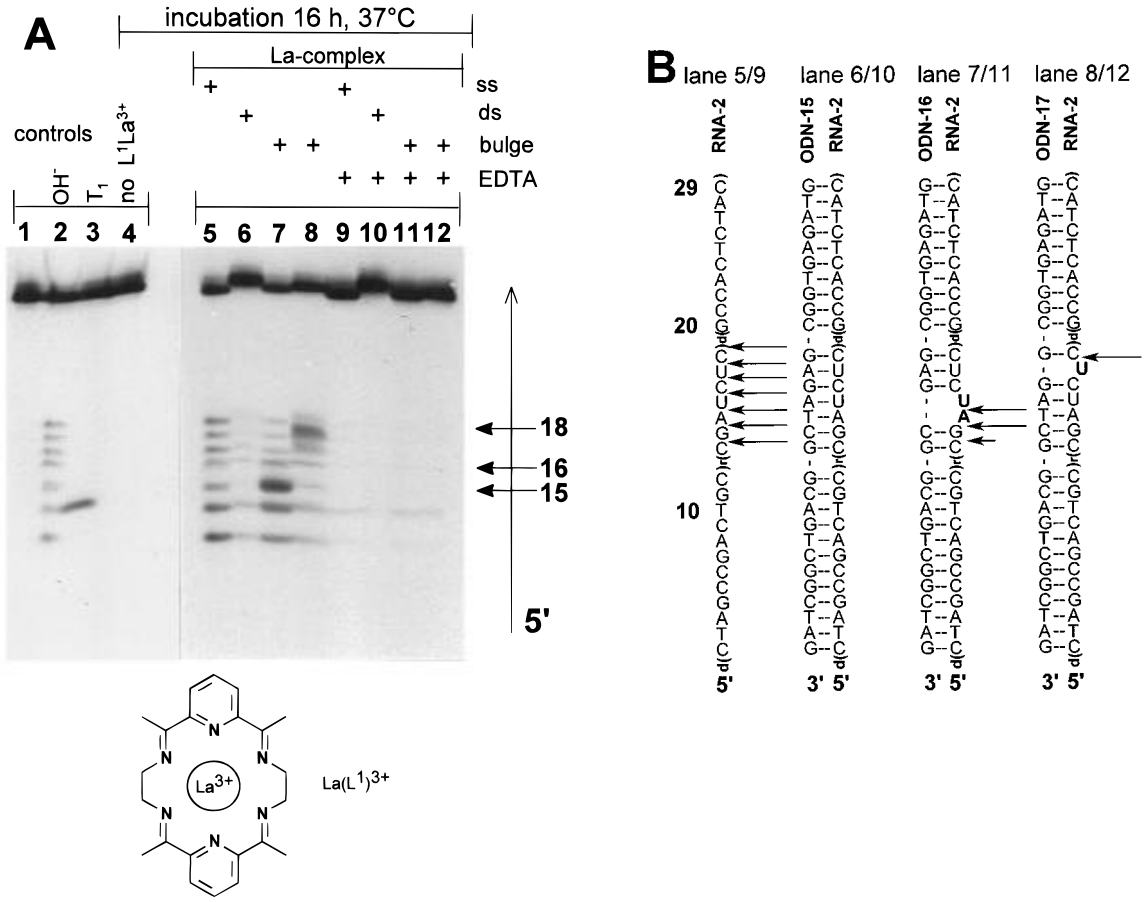

FIGURE 3: (A) Autoradiogram of a 12% denaturing polyacrylamide gel obtained after treatment of the 29 nt DNA/RNA/DNA oligonucleotide RNA-2 (29 nt, 5′-^{32}P-labeled) with the 0.4 mM lanthanum complex with or without EDTA in the presence of oligodeoxyribonucleotides (ODNs). The incubation was carried out at 37 °C for 16 h in a reaction mixture containing approximately 10−50 nM RNA-2 and 1 μM ODN in a buffer of 20 mM Tris-HCl at pH 7.4 in a total volume of 20 μL (lanes 4−12): lane 1, untreated RNA-2; lane 2, partial alkaline hydrolysis (sodium hydrogen carbonate at pH 10 for 20 min at 70 °C); lane 3, partial digestion with RNase T1; lane 4, buffer only; and lanes 5 and 9, no ODN added. In lanes 6−8 and 10−12, different ODNs were present: lanes 6 and 10, ODN-15, 29 nt, fully complementary to RNA-2; lanes 7 and 11, ODN-16, 27 nt, one double bulge at positions 15 and 16; and lanes 8 and 12, ODN-17, 28 nt, single bulge at position 18. In lanes 9−12, 10 mM EDTA was added. The arrows show the bulge positions. (B) Schematic presentation of the observed lanthanum complex [La(L^1)$^{3+}$]-promoted cleavage of RNA-2 (shown in Figure 3A) with the same lane counting. The positions of the bases are numbered counting from the 5′-end of the RNA-2 target. The cleavage sites are indicated by arrows of different lengths regarding the cleavage intensities. The bulged bases are depicted within the duplex. The deoxy and ribo sections of the target strand are denoted d and r, respectively. The formula of the lanthanum complex [La(L^1)$^{3+}$] is drawn below.

11 and ODN-12, which induce mismatches in RNA-1. Oligodeoxyribonucleotides were synthesized by phosphoramidite chemistry on an ABI Model 380B synthesiser, purified by denaturing polyacrylamide gel electrophoresis, electroeluted from gel slices, desalted by dialysis against water, and quantitated by absorbance at 260 nm using molar extinction coefficients according to the nearest-neighbor interaction calculation assuming no hypochromicity (Puglisi & Tinoco, 1989).

Labeling of Target RNA-1 and RNA-2. The transcript (RNA-1) was dephosphorylated in 50 μL of 20 mM Tris-HCl (pH 8.0) containing 1 mM magnesium chloride, 1 mM zinc chloride, 0.8 u/μL RNasin, and 0.02 u/μL calf intestinal phosphatase. Reaction mixtures were incubated for 20 min at 37 °C and adjusted to a 100 μL volume to a final concentration of 1 mM EDTA, 0.5% SDS, and 0.4 μg/μL proteinase K. The incubation was continued for 20 min. After phenol/chloroform/isoamyl alcohol (25:24:1, v/v/v) extraction and ethanol precipitation with 0.26 M sodium acetate (pH 7.0), the RNA was washed twice with 70% ethanol. One-fifth of the transcript was end-labeled in 20 μL of 50 mM Tris-HCl (pH 7.5) containing 10 mM magnesium chloride, 5 mM dithiothreitol, 2 u/μL RNasin, 0.75 μCi/μL (3000 Ci/mmol) [γ-^{32}P]ATP, and 0.2 u/μL T4 polynucleotide kinase. Reaction mixtures were incubated at 37 °C for 20 min, and after addition of 0.2 U/μL T4 polynucleotide kinase, the incubation was continued for 20 min. The end-labeled RNA was ethanol-precipitated with 2 M ammonium acetate, 10 mM EDTA, and 0.075 μg/μL glycogen and then dissolved in formamide/urea loading buffer (40% deionized formamide, 3.5 M urea, 10 mM EDTA, 0.02% xylene cyanol, and bromophenol blue) for separation on a 6% denaturing polyacrylamide gel. The visualized band was cut out, and the RNA was electroeluted in buffer (8.9 mM Tris, 8.9 mM boric acid, and 0.2 mM EDTA) with the Bio-Trap apparatus (Schleicher & Schuell) and ethanol-precipitated with 0.25 M sodium acetate and 0.2 μg/μL glycogen at pH 5.2. Synthetic RNA-2 (RNA/DNA chimeric oligonucleotide) was labeled and purified in a manner similar to that of the RNA-1 transcript. For each reaction with T4 polynucleotide kinase in a 20 μL volume, 100 pmol of substrate was incubated. The amount was counted with a Cerenkov protocol.

Cleavage Assay with Metal Ion and Metal Complex. Partial alkaline hydrolysis of RNAs was carried out with 0.2 M sodium hydrogen carbonate (pH 10) for 20 min at 70 °C.

Partial digestion of RNAs was carried out with RNase T_1 (10 u/μL) for 20 min at 70 °C in 7 M urea, 20 mM citric acid, and 1 mM EDTA. The standard reaction mixture (20 μL volume) for specific cleavage of RNA-1 by Mg^{2+} ions contained 2.5 mM magnesium chloride, 50 mM sodium borate (pH 8.0), and 0.1 M sodium acetate and was incubated for 16 h at 60 °C. For specific cleavage of RNA-2 by lanthanum complexes, the mixture contained 0.4 mM lanthanum complex and 20 mM Tris-HCl (pH 7.4 at 37 °C) and was incubated for 16 h at 37 °C. The RNAs estimated from the Cerenkov counting amounted to approximately 10−50 nM and the added ODNs to 1 μM. All mixtures were preincubated by heating to 85 °C for 1 min and slowly cooled to 37 °C before the 16 h incubation period. Reactions with RNA-1 were stopped by ethanol precipitation with 1.5 M ammonium acetate and analyzed with 10 μL of formamide/urea loading buffer by polyacrylamide gel electrophoresis on 10% sequencing gels. Reactions with RNA-2 were stopped by addition of 10 μL of formamide/urea loading buffer and analyzed by polyacrylamide gel electrophoresis on 12% sequencing gels.

Synthesis of La(III) Hexadentate−Schiff Base Macrocycle Complex [La(L^1)$^{3+}$] Acetate. Synthesis of La(III) hexadentate Schiff base macrocycle complex [La(L^1)$^{3+}$] acetate was carried out as described previously (DeCola et al., 1986). [La(L^1)$^{3+}$] acetate stock solutions [2 mM in 50 mM Tris-HCl (pH 7.7)] were stored at −80 °C to avoid hydrolysis of the complexes.

Generation of Model Structures. Molecular models of bulged RNA shown in Figure 5 were generated by means of a combined distance geometry and simulated annealing approach as described previously (Garbesi et al., 1993). All calculations were carried out on a SGI computer, using the InsightII-Discover package (BIOSYM) in conjunction with software for generating the restraint files. The structures were created with the positions of the bases held rigid in an A-type helix conformation. The geometric properties of the assumed stacking were translated into interatom distances and given as input for distance geometry calculations using the DGII program (Havel, 1991). The embedding was carried out in four dimensions. After the embedding, the structures were refined with 10 000 steps of simulated annealing. This provides a broad sampling of the sugar and the backbone conformations. In-line models were obtained by application of restraints between 2′-O and P (1.8−2.2 Å) and 2′-O and 5′-O (3.4−3.8 Å). The resulting structures were used as starting structures for molecular mechanics calculations under vacuum using the AMBER force field (Weiner et al., 1986). Electrostatic interactions were scaled by 4/*R*.

RESULTS

Oligoribonucleotides RNA-1 and RNA-2 were hybridized separately with oligodeoxynucleotides ODN-1−17 to give several different types of target structures for cleavage studies, including single-stranded RNA, double-stranded RNA, double-stranded structures containing bulged deoxy- and ribonucleotides, and mismatched base pairs.

RNA-1 was used as a target for cleavage promoted by the Mg^{2+} ions. Treatment with RNase T_1 under nondenaturing conditions exhibited no cleavage at guanines G-13, G-14, G-15, G-24, and G-25 (data not shown), confirming the presence of a self-complementary duplex region (the secondary structure prediction of RNA-1 by *FoldRNA* is depicted in Figure 1). In spite of this secondary structure, all of the antisense oligonucleotides targeted to this region were hybridized to their respective complementary sites.

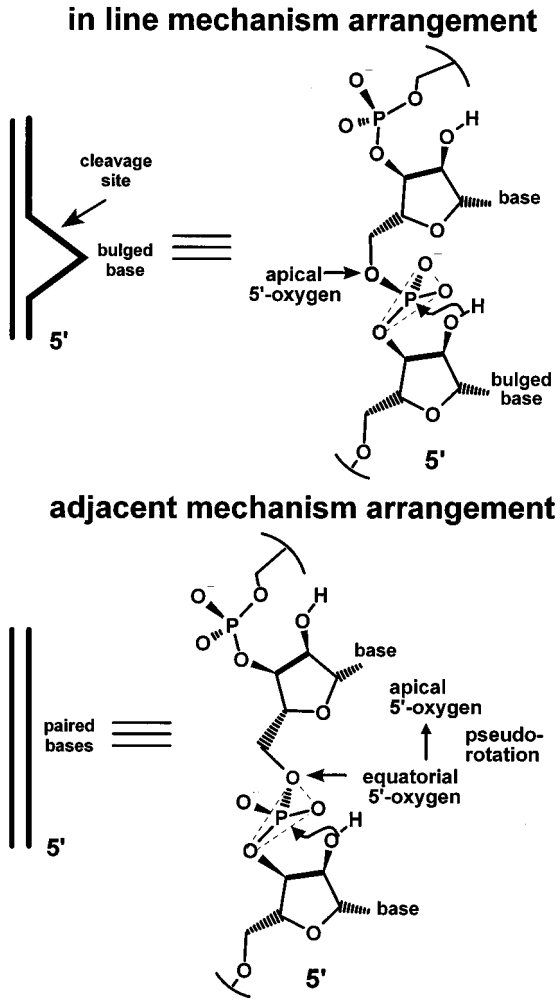

FIGURE 4: (Left) Schematic drawing of the bulged base cleavage site and normal paired bases in a duplex. (Right) Formulas displaying the preorientation of the attacking and leaving groups for the transesterification at a bulge in the RNA strand *versus* a fully complementary RNA strand. In the adjacent mechanism, after the initial 2′-oxygen attack, the 5′-oxygen has to pseudorotate from the equatorial position to the apical position before cleavage at the P−5′−O bond can occur.

In a first series of experiments, bulges containing one to four ribonucleotides were induced in the RNA strand by the appropriate choice of the base sequence of the antisense molecule. The calculated difference in melting temperature (ΔT_m) was approximately 5 °C lower for single bulges, 8−12 °C lower for two to four unpaired bases, and 18 °C lower for the four separated single bulges than for the fully complementary duplex ODN-1/RNA-1 (bases 1−30) (Freier et al., 1986; Jaeger et al., 1989; Longfellow et al., 1990). Reaction conditions (i.e. temperature, concentration, and pH) were controlled such that the promoted cleavage of the Mg^{2+} ion was sufficiently high for detection without disrupting the formed hybrid duplex. Single-stranded cleavage of the RNA in buffer alone at elevated temperatures was less pronounced than in the presence of the magnesium salts (Figure 2, lanes 4 and 5, respectively).

In the presence of Mg^{2+}, site specific cleavage of RNA-1 was seen predominantly at the 3′-side of the induced bulge (Figure 4) when hybridized to ODN-3−7 (Figure 2, lanes

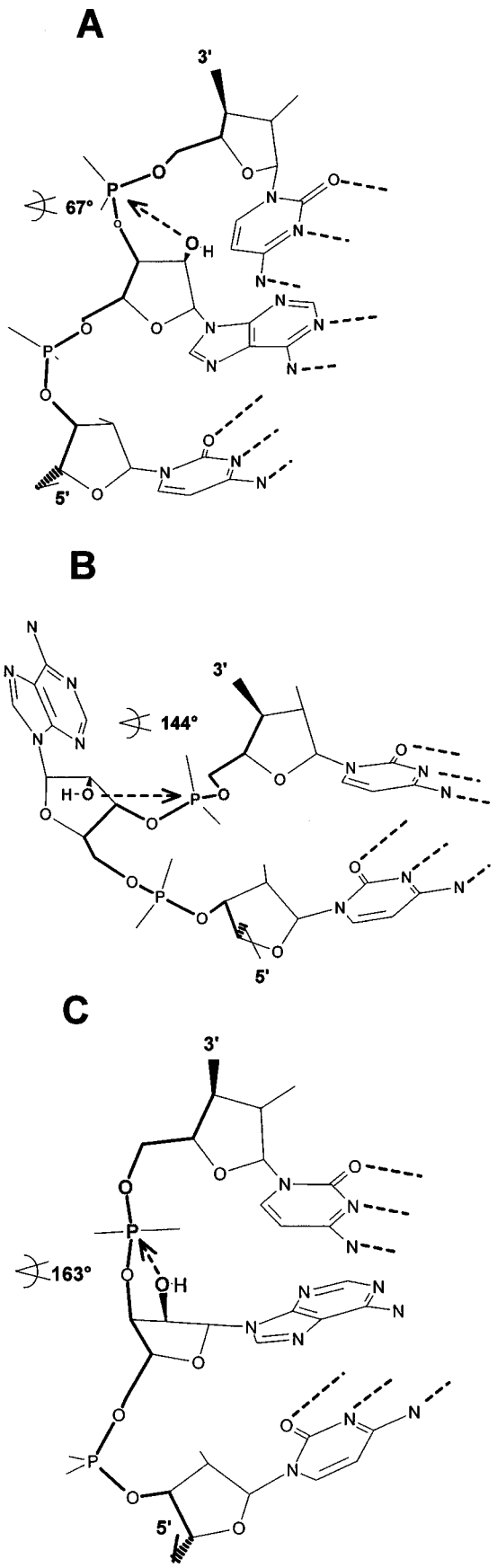

FIGURE 5: Comparison of the sugar−phosphate backbone of a ribotrinucleotide r(CAC) for regular duplex and in-line structures: (A) a normal A-type RNA duplex conformation, (B) a model for the in-line conformation of the looped-out base, and (C) a model for the in-line conformation of the stacked-in base. The 2′-O−P−5′-O angles are indicated. The in-line orientation is shown with arrows. The hydrogen bonds of the Watson−Crick base pairs are illustrated by dashed lines.

8−12, respectively). In most cases, secondary cleavage events were also observed one or even two positions on the 5′-side of the bulged nucleotide, i.e. at the bulged A-23 (Figure 2, lane 10). This behavior can be explained by the fact that the bulged nucleotide becomes more flexible after scission at the 3′-phosphodiester and therefore behaves like single strand at a dangling end. Another cleavage band, one nucleotide beyond the bulge on the 3′-side, was observed in the cases of the bulged C-10 and U-28 with ODN-3 and ODN-6, respectively (Figure 2, lanes 8 and 11, respectively). In both cases, this can be attributed to the effects of a weak duplex section composed of A·U/T base pairs on the 3′-side of the bulge (Ke & Wartell, 1995).

It was possible to induce cleavage at almost any chosen site of the target RNA. Hence, a one-base shift of the bulge in RNA-1 by the use of ODN-4 and ODN-7 resulted in the expected shifted cleavage bands (Figure 2, lanes 9 and 12, respectively). Even with four single bulged bases separated by a minimum of four base pairs (with ODN-6; Figure 2, lane 11), specific cleavage sites were induced. A minimum length of four paired bases at the end of a duplex was found to be necessary to stabilize the bulge under the reaction conditions (data not shown). Increasing the number of nucleotides in the bulge increased the cleavage window. Cleavage at two-base bulges induced, for example, with ODN-8 (Figure 2, lane 13) was as specific as that at single-base bulges. With loops of three and four unpaired bases, the expected widening of the cleavage window was observed. At the bulges induced by ODN-9 and ODN-10, this widening of the cleavage window occurred, in both cases, at flanking A·U/T base pair sites (Figure 2, lanes 14 and 15), as in the aforementioned example. Cleavage at four main sites was observed in the case of the three-base bulge, while seven bands were obtained with the four bulged bases (Figure 2, lanes 14 and 15). The kinetic development of these cleavage pattern of the bulge loop was not further examined. One plausible explanation is that this bulge loop behaves as a single-strand RNA with a certain amount of "breathing" at the single-strand−double-strand junction.

Prior hybridization of RNA-1 with complementary ODN-1 resulted in complete protection of the helical RNA region against cleavage by Mg^{2+} (Figure 2, lane 6). However, the observed protection region did not correlate exactly with the terminus of the duplex since cleavage was also observed among the last few bases at the junctions between the single strand and the double strand; the end of the protection zone varied from three nucleotides at the 5′-end to one nucleotide at the 3′-end (for clarity, see Figure 2B−D). These effects might be explained, on the one hand, by certain conformational preferences of the single strand close to the end of the duplex and, on the other hand, by the hybridization strength of the first few base pairs in the duplex.

The following rules were deduced from more than 35 different experiments (not all data shown) to predict the hydrolytic cleavage behavior at bulged RNA nucleotides. (i) Cleavages predominantly occur at the phosphodiester bond on the 3′-side of the bulged nucleotide. (ii) In most cases, secondary strand scissions occur at the phosphodiester on the 5′-side of the bulged nucleotide. (iii) Bulges that are flanked by two A·T or U·A base pairs on the 3′-side are also susceptible to cleavage. (iv) There is no difference in cleavage activity or specificity for the single bulged bases G, A, C, or U; the cleavage intensity was always in the same range and dependent on the neighboring sequences.

Other types of structural motifs were also investigated for cleavage activity. Placing a bulged nucleotide in the DNA (ODN-2) strand did not cause cleavage in the opposite RNA strand (Figure 2, lane 7). This observation implies that a single bulge in one strand has no significant effect on the nucleotide phosphodiesters in the opposite strand.

Distortions in the phosphodiester backbone caused by base pair mismatches were examined for cleavage reactivity (Figure 2, lanes 16 and 17). With a single mismatch, minor cleavage close to the mismatch was observed. Much stronger cleavage was detected for two adjacent mismatches, i.e. an internal loop (Figure 2, lane 17). The cleavage intensity and pattern induced with ODN-12 is comparable to that of the double-bulge cleavage (Figure 2, lane 13).

The two last examples (Figure 2, lanes 18 and 19) again show bulge-induced cleavage, where, due to the nearest-neighbor nucleotides, different bases can form the bulge (Figure 2D). Even in these cases, strand scission occurred as expected, where the flanking Watson−Crick base pairs were weakest. In the single-bulge case induced with ODN-13, cleavage occurs at position G-13, and in the case of the three-bulge bases induced with ODN-14, the cleavage was observed at positions C-19, G-18, and U-17. Examination of the cleavage pattern allows the predominant position of the bulge to be identified.

Experiments with the La(III) hexadentate−Schiff base macrocycle complex (L^1La^{3+}) acetate represent initial studies in the search for a suitable reagent that could be attached to antisense oligonucleotides for obtaining artificial nucleases. A chimeric oligonucleotide (RNA-2) containing an RNA window flanked by DNA sequences was used as the target molecule (Figure 3B). This model had the advantage of testing not only the cleavage of single-stranded RNA and DNA, as well as that of double-stranded RNA, but also the reaction at a bulge. Compared to Mg^{2+}, the complex (L^1La^{3+}) acetate showed very efficient cleavage at single-stranded as well as bulged ribonucleotides (Figure 3, lanes 5, 7, and 8, respectively), but under much milder reaction conditions (pH 7.2, 37 °C, and 16 h). Only by raising the concentration of the Mg^{2+} salts to 10 mM was it possible to achieve a cleavage as efficient as with 0.4 mM (L^1La^{3+}) complex at 37 °C (data not shown).

DISCUSSION

One goal of this study was to investigate how the effects of perturbations in the backbone of double-stranded RNA influence the ease with which this backbone undergoes a metal-catalyzed transesterification and cleavage of the strand with formation of 2′,3′-cyclic phosphate. In our case, the perturbation is caused by an unpaired base in the RNA strand of the RNA/DNA hybrid. We describe what is known about the backbone conformation of a bulged base, what consequence the conformation has for the in-line transesterification reaction resulting in cleavage, and finally how this could be usefully applied in antisense technology.

Structures of Bulged Bases. Although much has been written about the global structural changes in the topology of helices containing bulged nucleotides (Bhattacharyya & Lilly, 1989; Hsieh & Griffith, 1989; Bhattacharyya et al., 1990; Tang & Draper, 1990; Weeks & Crothers, 1993; Zacharias & Hagerman, 1995; Lilley, 1995), much less is known about the local structure at a bulge. Introduction of an unpaired base into an oligonucleotide duplex structure offers two possibilities for the placement of the nucleic base; either it is stacked into the helix, intercalating between the bases of its nearest neighbors, or it is looped out and consequently devoid of any stable stacking pattern. Only two crystal structures of a DNA/DNA and recently of a chimeric RNA/DNA duplex containing single unpaired deoxyadenosine have been published (Miller et al., 1988; Joshua-Tor et al., 1988, 1992; Portmann et al., 1996). Several DNA/DNA duplexes with bulges in solution have been investigated by NMR spectroscopy (Nikonowicz et al., 1990; Rosen et al., 1992a,b; Aboul-Ela et al., 1993). Studies of bulged RNAs, however, are sparse (van den Hoogen et al., 1988; Puglisi et al., 1992; Shen et al., 1995), and as yet, no structural data are available from a DNA/RNA duplex carrying a bulged base in the RNA strand. Early spectroscopic work has shown that it is easy for a bulged deoxy base to flip between the stacked-in and the looped-out arrangements, especially at higher temperatures. The relative populations for each state observed were reported to depend on the temperature. The proportion of stacked-in arrangements is higher at elevated temperatures (Kalnik et al., 1990; Morden & Maskos, 1993). In spite of this, cases of both looped-out and stacked-in bases at a bulge have been characterized in solution, and of these, purine bases are usually found stacked into the duplex whereas pyrimidine bases occupy looped-out positions.

Although it is not known whether a unique topology, looped-out or stacked-in, is necessary or favored for a facile transesterification reaction at the bulge, it is likely that conformational flipping from one form to the other can occur easily under the reaction conditions employed for this study. We observed no significant difference in cleavage reactivity between purine and pyrimidine bulges.

There is convincing evidence from various sources that the structural perturbations caused by an unpaired base within a duplex are confined to the immediate vicinity (±one nucleotide) of the bulged base in the same strand. For example, the aforementioned DNA/DNA crystal structure, which shows both the looped-out and the stacked-in forms of a bulged base in the same duplex, and the RNA/DNA chimera crystal structure with looped-out bases both display normal helical conformations for the phosphate groups of the nucleotides in the opposite strand (Joshua-Tor et al., 1992; Portmann et al., 1996). We obtained indirect experimental support for this latter observation (see Figure 2, lane 7); a bulged deoxyribonucleotide placed in the DNA strand of an RNA/DNA double helix did not induce cleavage at the opposite ribonucleotides of the RNA strand, indicating that the cleavage-stable helical conformation is maintained in the opposite strand.

Mechanisms for Transesterification and Detailed Conformation Consideration. Under a range of different reaction conditions, we observed that the placement of an unpaired, bulged ribonucleotide in a RNA/DNA duplex renders that nucleotide susceptible to cleavage at its phosphodiester. By contrast, its nearest neighbors, which maintain a typical helical conformation, like normal duplex RNA, are protected against scission. Comigration of the cleavage products on a sequencing gel (Figure 2) with the products from partial alkaline hydrolysis and partial treatment with RNase T_1 revealed that the cleavage product is 2′,3′-cyclic phosphate. This method was also used to establish the identity of cleavage products from Pb^{2+}- and Mn^{2+}-dependent ribozymes (Dange et al., 1990; Pan & Uhlenbeck, 1992; Van

Table 2: Backbone 2′-O−P−5′-O Angles and 2′-O−P Distances for Regular Duplexes and In-Line Structures

X-ray	bulge[b] (sti)	bulge[b] (lo)	bulge[c] (lo)	A-type[d] RNA/RNA	B-type[d] DNA/DNA	model	in-line bulge (lo)	in-line bulge (sti)
angle[a]	86°	132°	145°	67°	72°	angle	144°	163°
distance[a]	3.2	3.7	3.8	3.9	2.2	distance	3.7	2.3

[a] The distances between the two atoms 2′-O and P are given in angstroms. The angle is measured through space between the 2′O, P, and 5′-O atoms. The bulge types looped-out (lo) and stacked-in (sti) are given in parentheses. [b] DNA/DNA. [c] DNA/RNA chimera. [d] Average values.

Atta & Hecht, 1994). This intramolecular transesterification proceeds *via* nucleophilic attack by the 2′-oxygen at the phosphorus atom of the phosphodiester, giving a 5-ring intermediate/transition state with a trigonal−bipyramidal arrangement of the oxygen atoms around the central phosphorus atom. This intermediate subsequently collapses to yield the cyclic 2′,3′-phosphodiester product. Two mechanistic pathways are possible for this process (Brown et al., 1985). Where the attacking nucleophile, the leaving group, and the phosphorus atom form a 180° angle, the reaction occurs most readily by the so-called in-line mechanism. If this arrangement is not possible, then a slower adjacent mechanism with a higher activation energy operates (Figure 4). The latter necessitates, after the formation of a monoanionic pentacoordinate intermediate, a pseudorotation around the phosphorus to position the leaving group in an apical position before the bond scission can occur (Westheimer, 1968; Brown et al., 1985; Breslow & Xu, 1993; Kirby & Marriott, 1995; Perrin, 1995). A variety of nucleases and ribozymes (see examples of Table 1; Long & Uhlenbeck, 1993; van Tol et al., 1990) operate by the in-line mechanism, probably because of the low activation energy offered by this pathway. Even DNA specific nucleases make use of an in-line displacement by nucleophilic attack of water (Kim et al., 1990; Beese & Steitz, 1991; Weston et al., 1992).

To confirm the likelihood of an in-line mechanism facilitating cleavage at the bulged bases in our DNA/RNA duplexes, we studied the backbone conformation described in the X-ray structures (Joshua-Tor et al., 1992; Portmann et al., 1996) and one also obtained by molecular modeling (Table 2). In the crystal structures, the relevant angles were 86° for the stacked-in and both 132 and 145° for the looped-out states, respectively. Molecular modeling of stacked-in and looped-out examples were performed by a combined distance geometry and simulated annealing approach (described in Materials and Methods) for a trinucleotide r(CAC). To simulate an A-type helix, which is the accepted form for RNA/DNA hybrids (Chou et al., 1989; Egli et al., 1992; Salazar et al., 1993; Sanghani & Lavery, 1994), the terminal phosphodiesters were held rigid at the appropriate distance and the aromatic residue positions of the outer bases were fixed. With these restrictions, the conformational space spanned by the central (bulged) nucleotide was sampled rigorously. Several conformations describing an in-line orientation of the 2′-oxygen, the phosphorus atom, and the 5′-oxygen (2′-O−P−5′-O) were generated. All of these were found to be relatively low-energy conformers with respect to both the phosphate backbone and the riboses (Pearlman & Kim, 1988). A large range of different backbone torsion angles and sugar conformations was possible for the looped-out arrangement, while at least three conformers predisposed to an in-line reaction were generated for the stacked-in arrangement. Examples are displayed in Figure 5B,C, together with a model of r(CAC) in a perfect A-type helix (Figure 5A). In both the looped-out (Figure 5B) and the stacked-in arrangements (Figure 5C), the angles defined by 2′-O−P−5′-O are close to 180° (Table 2), which is ideal for the in-line displacement. This contrasts strongly with the 2′-O−P−5′-O angle of 67° observed for the regular A-type helix and the angle of 86° observed for the stacked-in base in the DNA/DNA structure. These energy calculations are rather simplified and do not take into account, for example, the influence of coordinated cations, which may stabilize some of the structures (Yarus, 1993; Uchimaru et al., 1993; Pyle, 1993). However, taken together with the data from the crystal structure, this is strong evidence that the bulged structures formed during our experiments can easily reach the necessary conformation for transesterification by the in-line mechanism, thus explaining the rapid cleavage reactions observed in the presence of metal catalysts. Furthermore, the model calculations suggest that cleavage can occur equally well from either a looped-out or a stacked-in state. Additional supporting evidence for this hypothesis is also available from a report of a faster transesterification/cleavage of 2′−5′-linked RNA compared to its natural 3′−5′-linked counterpart (Usher & McHale, 1976). Examination of a simple molecular model for this system showed that the 2′-5′ phosphodiester internucleotide bond indeed has a 2′-O−P−5′-O angle in the range of 150−165°, i.e. close to in-line, depending on the sugar pucker.

Our observation that double and multiple bulges are cleaved as efficiently as single bulges and the double mismatch (internal loop) is expected in view of the additional conformational freedom available to the phosphodiester backbone in these cases.

Energy Profile for RNA Cleavage at a Bulge and in the Duplex. The energy profile for the transesterification of a phosphodiester RNA is composed of several steps, depending on the mechanism (Taira et al., 1991; Gerlt, 1993; Uebayasi et al., 1994). For those reactions proceeding by an in-line mechanism, i.e. in the single strand or at the bulged site in a duplex, formation of a single high-energy intermediate is followed by collapse to the products (see Figure 6A). For reactions that cannot occur *via* the in-line pathway because of conformational restraints, i.e. transesterification in a duplex, pseudorotation is necessary. The energy profile for this pseudorotation is shown in Figure 6B. The magnitude of the activation energy required for the pseudorotation is unknown for reactions catalyzed by metal cation, though it was found to be 10−17 kcal/mol for an alkoxyphosphorane (Gorenstein, 1970). This barrier is probably relatively high, since, with the exception of lead salts, most metals are unable to lower the barrier sufficiently for pseudorotation (Brown et al., 1985), and hence, transesterification in the duplex cannot occur. Even though the reason for this behavior is unclear, one possibility might be the fact that, by either direct metal−oxygen coordination or protonation, lead salts sufficiently stabilize the pentacoordinate, dianionic intermediate to allow the pseudorotation, whereas magnesium and many other salts do not. Consequently, RNA is protected against

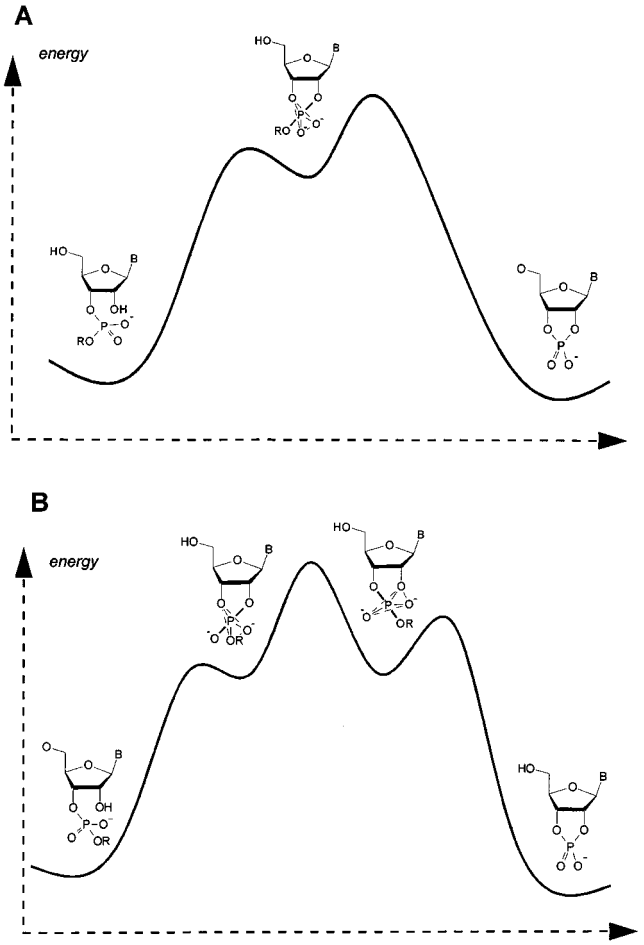

FIGURE 6: Energy profile of the transesterification pathway starting from a bulged base (A) or a duplex (B) situation in the RNA strand. In the duplex, the orientation of the 2′-oxygen allows no in-line pathway. For the dianionic intermediate/transition state, the pseudorotation barrier is drawn in panel B.

magnesium-catalyzed transesterification in the perfect duplex, where reaction is only allowed *via* pseudorotation. But in the single strand or at a bulged site, where an in-line path is easily attainable, transesterification is catalyzed.

We observed no reaction of double-stranded RNA in the presence of magnesium salts, even at elevated temperatures and concentrations. Lanthanum salts, however, did cause random cleavage of double-stranded RNA at 0.1 mM. One possibility is that lanthanide salts, like lead salts, are able to lower the activation energy for pseudorotation, possibly through their high (Lewis) acidity.

Our experiments and interpretations lead us to conclude that the most likely pathway for the transesterification reaction at a bulged site is the in-line mechanism.

Outlook. To date, to the best of our knowledge, no one has reported a chemical artificial ribonuclease which is capable of catalytic turnover, principally because cleavage of an RNA by an oligonucleotide conjugate typically occurs in single-stranded regions of the target, leading to product inhibition. To avoid this, it is necessary to cleave in the duplex formed between the artificial ribonuclease and the RNA. In this report, we have shown that cleavage in the duplex can be achieved under mild conditions with a suitable metal catalyst and a perturbed phosphodiester backbone. We have used bulged ribonucleotide bases in a RNA/antisense duplex as target sites for artificial nucleases (Hall et al., 1996). The final aim of this strategy is to be able to cleave in the RNA/antisense duplex at one or multiple sites to force a rapid product release from the oligonucleotide conjugate and thus offer the possibility of catalytic turnover. This possibility is currently being investigated.

ACKNOWLEDGMENT

We thank Judith Frei and Andrea Deichert for excellent technical assistance, Dr. Leemor Joshua-Tor, Dr. Stefan Portmann, and Dr. Martin Egli for the X-ray coordinates, and Prof. Witold Filipowicz for critical reading of the manuscript.

REFERENCES

Aboul-Ela, F., Murchie, A. I. H., Homans, S. W., & Lilly, D. M. J. (1993) *J. Mol. Biol. 229*, 173−179.
Altman, S., Kirsebom, L., & Talbot, W. (1993) *FASEB J. 7*, 7−14.
Altmann, K. H., Dean, N. M., Fabbro, D., Freier, S. M., Geiger, T., Häner, R., Hüsken, D., Martin, P., Monia, B. P., Müller, M., Natt, F., Nicklin, P., Phillips, J., Pieles, U., Sasmor, H., & Moser, H. E. (1996) *Chimia 50*, 168−176.
Amin, S., Morrow, J. R., Lake, C. H., & Churchill, M. R. (1994) *Angew. Chem., Int. Ed. Engl. 33*, 773−775.
Arni, R., Heinemann, U., Tokuoka, R., & Saenger, W. (1988) *J. Biol. Chem. 263*, 15358−15368.
Beese, L. J., & Steitz, T. A. (1991) *EMBO J. 10*, 25−33.
Bhattacharyya, A., & Lilley, D. M. J. (1989) *Nucleic Acids Res. 17*, 6821−6840.
Bhattacharyya, A., Murchie, A. I. H., & Lilley, D. M. J. (1990) *Nature 343*, 484−487.
Borah, B., Chen, C.-W., Egan, W., Miller, M., Wlodawer, A., & Cohen, J. S. (1985) *Biochemistry 24*, 2058−2067.
Breslow, R., & Huang, D. L. (1991) *Proc. Natl. Acad. Sci. U.S.A. 88*, 4080−4083.
Breslow, R., & Xu, R. (1993) *J. Am. Chem. Soc. 115*, 10705−10713.
Brown, R. S., Dewan, J. C., & Klug, A. (1985) *Biochemistry 24*, 4785−4801.
Cech, T. R., Herschlag, D., Piccirilli, J. A., & Pyle, A. M. (1992) *J. Biol. Chem. 267*, 17479−17482.
Chin, K. O. A., & Morrow, J. R. (1994) *Inorg. Chem. 33*, 5036−5041.
Chou, S.-H., Flynn, P., & Reid, B. (1989) *Biochemistry 28*, 2435−2443.
Cotton, F. A., Hazen, E. E., Jr., & Legg, M. J. (1979) *Proc. Natl. Acad. Sci. U.S.A. 76*, 2551−2555.
Crooke, S. T. (1994) *Antisense Res. Dev. 4*, 145−146.
Cuchillo, C. M., Parés, X., Guasch, A., Barman, T., Travers, F., & Nogués, M. V. (1993) *FEBS Lett. 333*, 207−210.
Dange, V., van Atta, R. B., & Hecht, S. M. (1990) *Science 248*, 585−588.
Davies, J. F., Hostomska, Z., Hostomsky, Z., Jordan, S., & Mathews, D. A. (1991) *Science 252*, 88−95.
De Mesmaeker, A., Häner, R., Martin, P., & Moser, H. E. (1995) *Acc. Chem. Res. 28*, 366−374.
DeCola, L., Samailes, D. L., & Vallarino, L. M. (1986) *Inorg. Chem. 25*, 1729−1732.
Eftink, M. R., & Biltonen, R. L. (1983a) *Biochemistry 22*, 5123−5134.
Eftink, M. R., & Biltonen, R. L. (1983b) *Biochemistry 22*, 5134−5140.
Eftink, M. R., & Biltonen, R. L. (1983c) *Biochemistry 22*, 5140−5150.
Egli, M., Usman, N., Zhang, S., & Rich, A. (1992) *Proc. Natl. Acad. Sci. U.S.A. 89*, 534−538.
Eichhorn, G. L., & Butzow, J. J. (1965) *Biopolymers 3*, 79−94.
Field, A. K., & Goodchild, J. (1995) *Exp. Opin. Invest. Drugs 4*, 799−821.
Freier, S. M., Kierzek, R., Jaeger, J. A., Sugimoto, N., Caruthers, M. H., Neilson, T., & Turner, D. H. (1986) *Proc. Natl. Acad. Sci. U.S.A. 83*, 9373−9377.
Garbesi, A., Capopbianco, M. L., Colonna, F. P., Tondelli, L., Arcamone, F., Manzini, G., Hilbers, C. W., Aelen, J. M. E., & Blommers, M. J. J. (1993) *Nucleic Acids Res. 21*, 4159−4165.

Gerlt, J. A. (1993) in *Nucleases Second Edition* (Linn, S. M., Lloyd, R. S., & Roberts, R. J., Eds.) pp 1−34, Cold Spring Harbor Laboratory Press, Plainview, NY.
Goodall, G. J., & Filipowicz, W. (1989) *Cell 58*, 473−483.
Gorenstein, D. (1970) *J. Am. Chem. Soc. 92*, 644−650.
Gornicki, P., Baudin, F., Romby, P., Wiewiorowski, M., Kryzosiak, W., Ebel, J. P., Ehresmann, C., & Ehresmann, B. (1989) *J. Biomol. Struct. Dyn. 6*, 971−983.
Hall, J., Hüsken, D., Pieles, U., Moser, H. E., & Häner, R. (1994) *Chem. Biol. 1*, 185−190.
Hall, J., Hüsken, D., & Häner, R. (1996) *Nucleic Acids Res. 24*, 3522−2526.
Häner, R., Hall, J., Hüsken, D., & Moser, H. E. (1996) in *DNA and RNA Cleavers and Chemotherapy of Cancer and Viral Diseases* (Meunier, B., Ed.) NATO ASI Series, Vol. 479, pp 307−320, Kluwer Academic Publishers, Dordrecht, The Netherlands.
Havel, T. F. (1991) *Prog. Biophys. Mol. Biol. 56*, 43−78.
Hayashi, N., Takeda, N., Shiiba, T., Yashiro, M., Watanabe, K., & Komiyama, M. (1993) *Inorg. Chem. 32*, 5899−5900.
Herschlag, D., & Cech, T. R. (1990) *Nature 344*, 405−409.
Hjalt, T. Å. H., & Wagner, E. G. H. (1995) *Nucleic Acids Res. 23*, 571−579.
Hsieh, C.-H., & Griffith, J. D. (1989) *Proc. Natl. Acad. Sci. U.S.A. 86*, 4833−4837.
Jaeger, J. A., Turner, D. H., & Zucker, M. (1989) *Proc. Natl. Acad. Sci. U.S.A. 86*, 7706−7710.
Joshua-Tor, L., Rabinovich, D., Hope, H., Frolow, F., Appella, E., & Sussman, J. L. (1988) *Nature 334*, 82−84.
Joshua-Tor, L., Frolow, F., Appella, E., Hope, H., Rabinovich, D., & Sussman, J. L. (1992) *J. Mol. Biol. 225*, 397−431.
Kalnik, M. W., Norman, D. G., Li, B. F., Swann, P. F., & Patel, D. J. (1990) *J. Biol. Chem. 265*, 636−647.
Katayanagi, K., Miyagawa, M., Matsushima, M., Ishikawa, M., Kanaya, S., Nakamura, H., Ikehara, M., Matsuzaki, T., & Morikawa, K. (1992) *J. Mol. Biol. 223*, 1029−1052.
Ke, S. H., & Wartell, R. M. (1995) *Biochemistry 34*, 4593−4600.
Kim, Y., Grable, J. C., Love, R., Greene, P., & Rosenberg, J. M. (1990) *Science 249*, 1307−1309.
Kirby, A. J., & Marriott, R. E. (1995) *J. Am. Chem. Soc. 117*, 833−834.
Kolasa, K. A., Morrow, J. R., & Sharma, A. P. (1993) *Inorg. Chem. 32*, 3983−3984.
Kuusela, S., & Lönnberg, H. (1994) *J. Chem. Soc., Perkin Trans. 2*, 2301−2306.
Li, H.-L., Chelladurai, B. S., Zhang, K., & Nicholson, A. W. (1993) *Nucleic Acids Res. 21*, 1919−1925.
Lilley, D. M. J. (1995) *Proc. Natl. Acad. Sci. U.S.A. 92*, 7140−7142.
Loll, P., & Lattman, E. E. (1989) *Proteins: Struct., Funct., Genet. 5*, 183−201.
Long, D. M., & Uhlenbeck, O. C. (1993) *FASEB J. 7*, 25−30.
Longfellow, C. E., Kierzek, R., & Turner, D. H. (1990) *Biochemistry 29*, 278−285.
Magda, D., Miller, R. A., Sessler, J. L., & Iverson, B. L. (1994) *J. Am. Chem. Soc. 116*, 7439−7440.
Matsumura, K., Endo, M., & Komiyama, M. (1994) *J. Chem. Soc., Chem. Commun.*, 2019−2020.
Matsuo, M., Yokogawa, T., Nishikawa, K., Watanabe, K., & Okada, N. (1995) *J. Biol. Chem. 270*, 10097−10104.
Miller, M., Harrison, R. W., Wlodower, A., Apella, E., & Sussman, J. L. (1988) *Nature 334*, 85−86.
Morden, K. M., & Maskos, K. (1993) *Biopolymers 33*, 27−36.
Morrow, J. R., & Shelton, V. M. (1994) *New J. Chem. 18*, 371−375.
Morrow, J. R., Buttrey, L. A., Shelton, V. M., & Berback, K. A. (1992) *J. Am. Chem. Soc. 114*, 1903−1905.
Nikonowicz, E. P., Meadows, R. P., & Gorenstein, D. G. (1990) *Biochemisty 29*, 4193−4204.
Oda, Y., Yoshida, M., & Kanaya, S. (1993) *J. Biol. Chem. 268*, 88−92.
Pan, T., & Uhlenbeck, O. C. (1992) *Nature 358*, 560−563.
Pearlman, D. A., & Kim, S.-H. (1988) *Biopolymers 27*, 59−77.
Perrin, C. L. (1995) *J. Org. Chem. 60*, 1239−1243.
Pley, H. W., Flaherty, K. M., & McKay, D. B. (1994) *Nature 372*, 68−74.
Portman, S., Grimm, S., Workman, C., Usman, N., & Egli, M. (1996) *Chem. Biol. 3*, 173−184.
Puglisi, J. D., & Tinoco, I., Jr. (1989) *Methods Enzymol. 180*, 304−325.
Puglisi, J. D., Tan, R., Calna, B. J., Frankel, A. D., & Williamson, J. R. (1992) *Science 257*, 76−80.
Pyle, A. M. (1993) *Science 261*, 709−714.
Robertson, D. L., & Joyce, G. F. (1990) *Nature 344*, 467−468.
Rosen, M. A., Live, D., & Patel, D. J. (1992a) *Biochemistry 31*, 4004−4014.
Rosen, M. A., Shapiro, L., & Patel, D. J. (1992b) *Biochemistry 31*, 4015−4026.
Salazar, M., Fedoroff, O. Y., Miller, J. M., Ribeiro, N. S., & Reid, B. R. (1993) *Biochemistry 32*, 4207−4215.
Sanghani, S. R., & Lavery, R. (1994) *Nucleic Acids Res. 22*, 1444−1449.
Schneider, H.-J., Rammo, J., & Hettich, R. (1993) *Angew. Chem. 105*, 1773−1776.
Scott, W. G., Finch, J. T., & Klug, A. (1995) *Cell 81*, 991−1002.
Shen, L. X., Cai, Z., & Tinoco, I., Jr. (1995) *FASEB J. 9*, 1023−1033.
Taira, K., Uchimaru, T., Tanabe, K., Uebayasi, M., & Nishikawa, S. (1991) *Nucleic Acids Res. 19*, 2747−2753.
Tang, R. S., & Drapper, D. E. (1990) *Biochemistry 29*, 5232−5237.
Uchimaru, T., Uebayasi, M., Tanabe, K., & Taira, K. (1993) *FASEB J. 7*, 137−142.
Uebayasi, M., Uchimaru, T., Koguma, T., Sawata, S., Shimayama, T., & Taira, K. (1994) *J. Org. Chem. 59*, 7414−7420.
Usher, D. A., & McHale, A. H. (1976) *Proc. Natl. Acad. Sci. U.S.A. 73*, 1149−1153.
Van Atta, R. B., & Hecht, S. M. (1994) in *Models in inorganic Biochemistry* (Eichhorn, G. L., & Marzilli, L. G., Eds.) pp 2−40, PTR Prentice Hall, Englewood Cliffs, NJ.
Van den Hoogen, Y. T., van Beuzekom, A. A., de Vroom, E., van der Macel, G. A., van Boom, J. H., & Altona, C. (1988) *Nucleic Acids Res. 16*, 5013−5030.
Van Tol, H., Buzayan, J. M., Feldstein, P. A., Eckstein, F., & Bruening, G. (1990) *Nucleic Acids Res. 18*, 1971−1975.
Weeks, K. M., & Crothers, D. M. (1993) *Science 261*, 1574−1577.
Weiner, D. J., Kollman, P. A., Nguyen, D. T., & Case, D. A. (1986) *J. Comput. Chem. 7*, 230−235.
Westheimer, F. H. (1968) *Acc. Chem. Res. 1*, 70−78.
Weston, S. A., Lahm, A., & Suck, D. (1992) *J. Mol. Biol. 226*, 1237−1256.
Winkler, F. K., Banner, D. W., Oefner, C., Tsernoglou, D., Brown, R. S., Heathman, S. P., Bryan, R. K., Martin, P. D., Petratos, K., & Wilson, K. S. (1993) *EMBO J. 12*, 1781−1795.
Wyatt, J. R., & Walker, G. T. (1989) *Nucleic Acids Res. 17*, 7833−7842.
Yang, W., Hendrickson, W. A., Crouch, R. J., & Satow, Y. (1990) *Science 249*, 1398−1405.
Yarus, M. (1993) *FASEB J. 7*, 31−39.
Zacharias, M., & Hagerman, P. J. (1995) *J. Mol. Biol. 247*, 486−500.
Zuker, M. (1989) *Methods Enzymol. 180*, 262−288.

BI961700C